JGR Earth Surface

RESEARCH ARTICLE
10.1029/2021JF006153

Does Load-Induced Shallow Subsidence Inhibit Delta Growth?

E. L. Chamberlain[1,2], Z. Shen[3], W. Kim[4], S. McKinley[3], S. Anderson[3], and T. E. Törnqvist[1]

[1]Department of Earth and Environmental Sciences, Tulane University, New Orleans, LA, USA, [2]Soil Geography and Landscape Group and Netherlands Centre for Luminescence dating of Wageningen University, Wageningen, The Netherlands, [3]Department of Marine Science, Coastal Carolina University, Conway, SC, USA, [4]Department of Earth System Sciences, Yonsei University, Seoul, Republic of Korea

Key Points:

- Mouth-bar surfaces are common stratigraphic features in river-dominated deltas that represent an unexplored relative sea-level indicator
- Bayfloor muds may be more vulnerable to load-induced sediment compaction than peats in the Mississippi Delta
- Load-induced subsidence has a limited impact on delta progradation and may stabilize distributary channels

Supporting Information:

Supporting Information may be found in the online version of this article.

Correspondence to:

E. L. Chamberlain and W. Kim,
liz.chamberlain@wur.nl;
delta@yonsei.ac.kr

Citation:

Chamberlain, E. L., Shen, Z., Kim, W., McKinley, S., Anderson, S., & Törnqvist, T. E. (2021). Does load-induced shallow subsidence inhibit delta growth? *Journal of Geophysical Research: Earth Surface*, *126*, e2021JF006153. https://doi.org/10.1029/2021JF006153

Received 6 MAR 2021
Accepted 23 OCT 2021

Author Contributions:

Conceptualization: E. L. Chamberlain, Z. Shen, W. Kim, T. E. Törnqvist
Data curation: E. L. Chamberlain
Formal analysis: E. L. Chamberlain, Z. Shen, W. Kim, S. McKinley, S. Anderson, T. E. Törnqvist
Funding acquisition: E. L. Chamberlain, Z. Shen, W. Kim, T. E. Törnqvist

Abstract The ability of deltas to persist by building new land is critical to maintaining these vital ecologic environments that are often home to major economic and population centers. However, the deposition of land-building sediment triggers load-induced shallow subsidence which may undermine the effectiveness of natural and engineered emergent landforms. Here, we present a new method to quantify shallow subsidence in a 6,000–8,000 km^2 relict bayhead delta of the Mississippi Delta using the mouth bar to overbank stratigraphic boundary that formed near sea level, temporally constrained by optically stimulated luminescence dating. Vertical displacement rates at this boundary, averaged over 750–1,500 years, are on the order of a few mm/yr. Total subsidence scales to ~50% of the thickness of overlying deposits, significantly greater than the 28%–35% loss estimated for inland localities underlain by peat, indicating that bay muds in the study area are more compaction-prone than terrestrial organic-rich deposits. Modeling shows a modest reduction of ~13% in deltaic land-area gain under a realistic compaction scenario for 1,000 years of simulated delta progradation, compared to a no-compaction scenario. Our findings indicate that load-driven compaction does not majorly hinder land-area gain and may in fact promote long-term growth at engineered sediment diversions through channel maintenance driven by compaction, thereby adding further support to this restoration strategy.

Plain Language Summary Deltas naturally lose elevation with time, and this loss must be balanced by new deposition or growth to maintain the land area. However, the deposition of sand and mud may drive further elevation loss due to its weight acting on underlying deposits. We use a new method to extract information about the relationship between sediment loading and elevation loss using the sedimentary archive of an abandoned lobe in the Mississippi Delta. We show that coastal regions characterized by delta growth into open water, like our study area, are particularly prone to elevation loss. Nevertheless, we find that engineering solutions to build new land in deltas are still viable.

1. Introduction

Despite a reduction in the sediment flux from continents to oceans on a global scale (Syvitski et al., 2005), many river deltas have continued to grow in recent decades (Nienhuis et al., 2020). However, it is unlikely that this growth can be sustained under future scenarios of relative sea-level rise (RSLR), in part due to the commonly high subsidence rates in deltas. RSLR is a major threat to the sustainability of these ecologically, economically, and culturally significant regions (e.g., Bijlsma et al., 1996; Ericson et al., 2006; Higgins, 2016; Milliman & Haq, 1996; Shirzaei et al., 2021). While it is well-documented that compaction of shallow Holocene deposits triggered by sediment loading is a major contributing process (e.g., Jelgersma, 1996; Mazzotti et al., 2009; Teatini et al., 2011; Törnqvist et al., 2008; Zoccarato et al., 2018), a lack of empirical evidence on the compressibility of various deltaic facies hinders our ability to predict future subsidence rates and their spatiotemporal variability. A better understanding of load-induced shallow subsidence is needed to assess whether deltas will maintain their sustainability by creating new land through progradation or whether short-term elevation and land-area gains may be lost to subsidence driven by the deposition of new sediment.

Investigation: E. L. Chamberlain, Z. Shen, W. Kim, S. McKinley, S. Anderson, T. E. Törnqvist
Methodology: E. L. Chamberlain, Z. Shen, W. Kim, T. E. Törnqvist
Project Administration: T. E. Törnqvist
Resources: T. E. Törnqvist
Supervision: T. E. Törnqvist
Validation: E. L. Chamberlain, Z. Shen, W. Kim, T. E. Törnqvist
Visualization: E. L. Chamberlain, Z. Shen, W. Kim, S. McKinley, S. Anderson, T. E. Törnqvist
Writing – original draft: E. L. Chamberlain, Z. Shen, W. Kim, T. E. Törnqvist
Writing – review & editing: E. L. Chamberlain, Z. Shen, W. Kim, T. E. Törnqvist

Although wetlands can aggrade to maintain delta-plain elevation, the net growth of deltaic land is fundamentally tied to clastic deposition in open water, including estuarine bays. Still, coastal subsidence research has historically emphasized the importance of organic-rich portions of deltas where the subsidence risk is regarded as high due to the propensity of peat to oxidize and compact (e.g., Kaye & Barghoorn, 1964; Van Asselen et al., 2009). In the Mississippi Delta, the target of our study, the majority of research into shallow subsidence has focused on organic-rich (paleo) wetlands (Cahoon et al., 1995; Jankowski et al., 2017; Morton et al., 2006; Törnqvist et al., 2008). For example, the large network of rod surface-elevation tables (e.g., Webb et al., 2013) emplaced for wetland elevation-change monitoring (Steyer et al., 2003) enables instrumental-timescale evaluation of shallow subsidence, and peat beds preserved in the stratigraphic record are widely used sea-level or paleo-groundwater-table indicators that enable evaluating pre-instrumental rates of subsidence (Törnqvist et al., 2006). As such, there is a significant void of methodology as to how to determine subsidence in estuarine open-water environments where clastic sedimentation dominates.

Satisfying this knowledge gap is critical to determining the viability of coastal restoration initiatives, both for our study area and for coastal communities worldwide that are endangered by subsidence (Shirzaei et al., 2021). Over the past century, the Mississippi Delta has experienced net land loss at an average rate of 45 km^2/yr (Couvillion et al., 2017). Harnessing the Mississippi River's natural ability to build land through sediment diversions is a key component of a 50 billion dollar coastal management strategy outlined in the Louisiana Coastal Master Plan that aims to offset historic land losses (CPRA, 2017). Lessons learned from this strategy may be applicable to coastal management initiatives worldwide. Little is known about how muddy substrates at diversion sites, which are planned mainly for open-water estuarine bays, may respond to loading with sediment and the degree to which load-driven shallow subsidence may inhibit land growth.

Here, we apply a new method to quantify subsidence of a bayhead delta that built into a large estuarine bay using the chronostratigraphic record of the Lafourche subdelta of the Mississippi Delta (Figure 1). The emergence of the 6,000–8,000 km^2 bayhead portion of the Lafourche subdelta from 1.6 to 0.6 ka was recorded as a ubiquitous succession of shell-rich bay floor, laminated delta front, sandy mouth bar, and mud-dominated overbank deposits (Chamberlain et al., 2018; Figure 2a). We obtain subsidence values using the present-day depths and previously determined optically stimulated luminescence (OSL) ages (Chamberlain et al., 2018) of a stratigraphic boundary within this succession that we introduce as a novel relative sea-level (RSL) indicator. We apply our findings by means of a modified delta growth model (Kim, Dai, et al., 2009) to evaluate the potential effects of load-induced subsidence on delta progradation and land building. Our findings also shed light on the predominant drivers of deltaic subsidence which has been a contentious topic in the Mississippi Delta (e.g., Allison et al., 2016; Dokka et al., 2006; Kolker et al., 2011; Morton et al., 2006; Törnqvist et al., 2008, 2006). Figure 3 gives an overview of potential drivers of deltaic RSLR, including the various processes contributing to subsidence, and whether our method captures them.

2. Methods and Study Area

2.1. A New Method for Measuring Subsidence

Mouth bars consist mainly of sand deposited at the river mouth that aggrades to fill the accommodation created by RSLR (Figure 2a; Edmonds & Slingerland, 2007; Wright, 1977). As the top of the mouth bar approaches sea level, currents become less able to transport sand to the bar top and colonization by vegetation enhances the trapping of fine-grained sediments (Olliver & Edmonds, 2017; Paola et al., 2011). This produces an abrupt lithofacies change from sand to mud, referred to herein as the mouth bar to overbank (M-O) boundary (Figure 4). A survey of the Wax Lake Delta (Figure 1), an actively prograding bayhead delta within the Mississippi Delta, suggests that the M-O boundary corresponds to a transition from mouth bar to intertidal flat which is related to coeval sea level with a mean lower quartile formation elevation of -0.4 ± 0.2 m NAVD 88 (Olliver & Edmonds, 2017). We take this lower quartile as the elevation of the modern M-O boundary, assuming that higher intertidal flat elevations are due to sediment accretion above this boundary. Previous work has also related mouth-bar tops to the mean low water tidal datum (Wellner et al., 2005) and more broadly to sea level (Fisk et al., 1954; Roberts et al., 1997; Shen & Mauz, 2012), but without specific values for the elevation of this boundary. It is likely that the tidal range in this region has not changed significantly over the late Holocene (Hill et al., 2011).

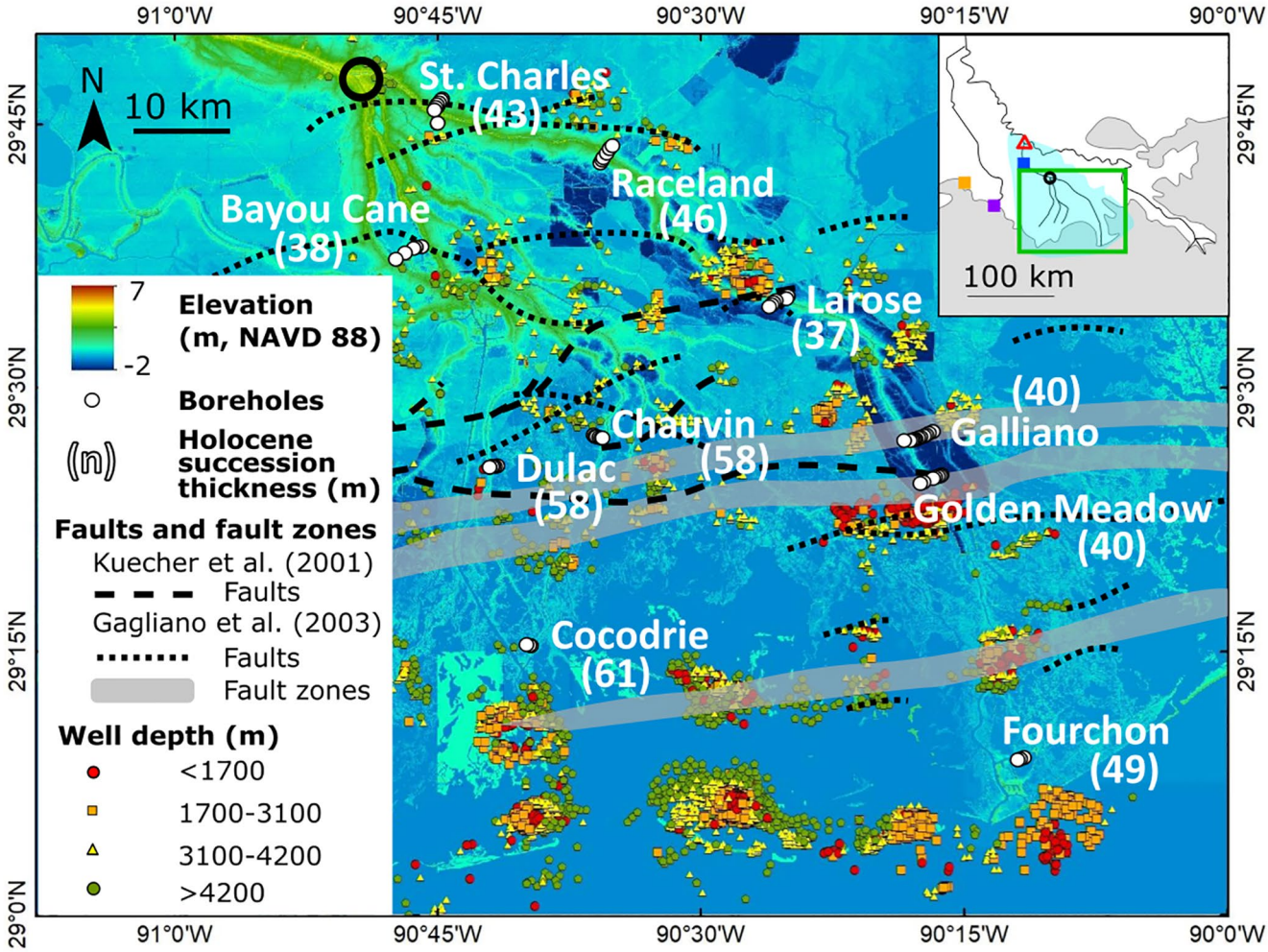

Figure 1. The location of cross-sections relative to Holocene succession thickness (Heinrich et al., 2015), oil- and gas-well depth (http://www.sonris.com/), and faults and fault zones mapped by Gagliano et al. (2003) and Kuecher et al. (2001). The bayhead-delta apex is indicated by the open black circle. The inset shows the location of the study area (green box) within the Lafourche subdelta (blue shaded region), the Lafourche-Modern avulsion site (red open triangle), the study areas of González and Törnqvist (2009) (orange box) and Törnqvist et al. (2008) (blue box), and the Wax Lake Delta (purple box). Additional information about oil and gas production is provided in Supporting Information S1.

Because the M-O boundary can be related to sea level and is a common stratigraphic boundary in river-dominated deltas, as well as in other coastal depositional systems such as tidal point bars overlain by marsh deposits (Brivio et al., 2016), it provides a valuable and as of yet unexplored RSL indicator. A similar innovation was conceptualized by Fisk et al. (1954), however, the chronologic and RSL data needed to apply their insight were lacking in the 1950s. Here, we use stratigraphic data in combination with OSL ages (Chamberlain et al., 2018) that capture the timing of formation of the M-O boundary, and an established record of compaction-free RSLR in the Mississippi Delta (González & Törnqvist, 2009; Törnqvist et al., 2006) to quantify cumulative subsidence. This is expressed as the net change in elevation of the M-O boundary (ΔE), calculated as:

$$\Delta E = \left(E_1 - E_0\right) + \Delta\mathrm{RSL} \quad (1)$$

In Equation 1, E_1 is the present-day elevation of the M-O boundary from borehole data with 0.1 m uncertainty for land surface elevation determined by LiDAR (Cunningham et al., 2004; Gesch, 2018) and a unidirectional 2% uncertainty (that is, 2% potential shortening) for depth overestimation due to non-vertical drilling. E_0 is the elevation at which the M-O boundary formed with respect to coeval sea level (Olliver & Edmonds, 2017). ΔRSL is the change in RSL since the time of M-O boundary formation (Figure 2b) with

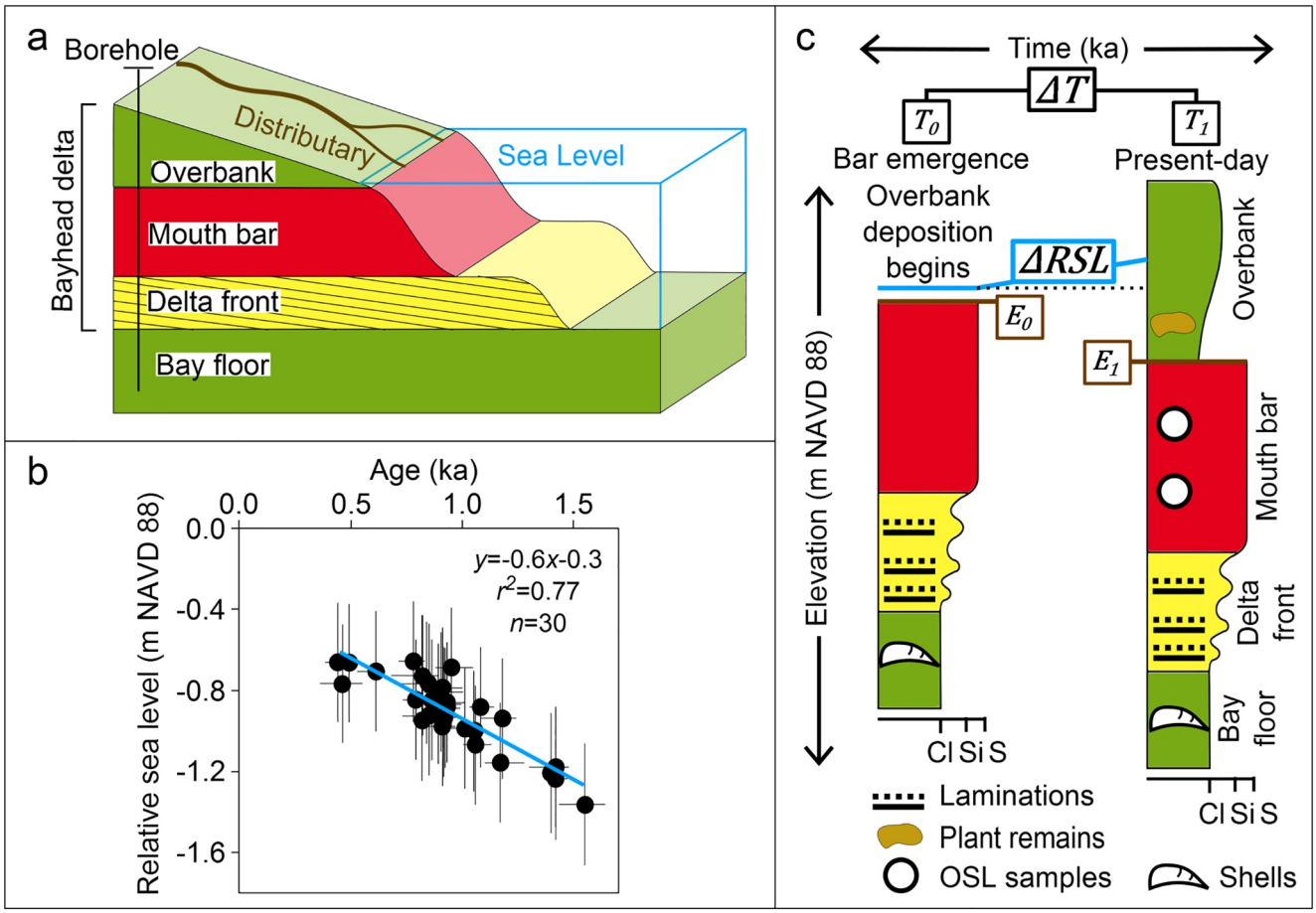

Figure 2. (a) The stratigraphic record of bayhead deltas can be generalized as bay floor clay overlain by delta front silt, then mouth bar sand, capped by mud-dominated overbank deposits that thin seaward (modified from Chamberlain et al., 2018). The mouth bar to overbank (M-O) boundary forms in relation to sea level (Fisk et al., 1954; Olliver & Edmonds, 2017; Roberts et al., 1997; Shen & Mauz, 2012; Wellner et al., 2005). Note that this cartoon does not consider compaction. (b) Compaction-free RSLR during the time of Lafourche subdelta progradation (after González & Törnqvist, 2009; Törnqvist et al., 2006). (c) Method for calculating subsidence uses the change in elevation of the M-O boundary (ΔE) from time of formation (E_0) to present (E_1), relative to NAVD 88 and corrected for RSLR (ΔRSL) since the time of M-O boundary formation (T_0) obtained from OSL dating of the mouth-bar deposits (Chamberlain et al., 2018).

	Drivers of deltaic relative sea-level rise	Key references	Captured by our method?	Comments
Subsidence	Compaction	Törnqvist et al. (2008) Meckel et al. (2006)	YES	Occurs over various depth scales; compaction of uppermost strata (above M-O boundary) not captured by our method
Subsidence	Fluid Extraction	Morton et al. (2006)	YES	Study sites selected away from extraction hotspots
Subsidence	Faulting	Hopkins et al. (2021) Frederick et al. (2019) Kuecher et al. (2001)	YES	May have very locally specific effects not captured by our site selection
Subsidence	Glacial isostatic adjustment	Love et al. (2016)	NO	Removed by subtraction of *ΔRSL*
Subsidence	Sedimentary isostatic adjustment	Wolstencroft et al. (2014) Yu et al. (2012)	NO	Removed by subtraction of *ΔRSL*
Sea level	Geocentric sea-level rise	Hijma et al. (2015) González & Törnqvist (2009) Törnqvist et al. (2006)	NO	Removed by subtraction of *ΔRSL*

Figure 3. Drivers of deltaic relative sea-level rise, and whether they are captured by our method. Key references are specific to the Mississippi Delta.

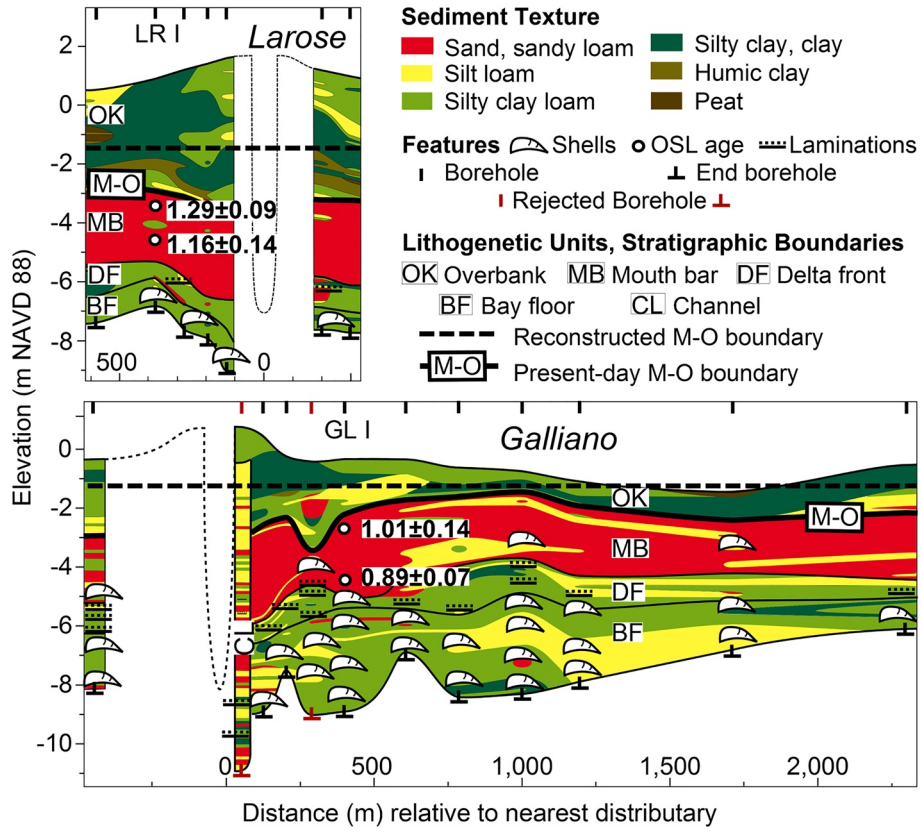

Figure 4. Two examples of Lafourche bayhead delta stratigraphy in coast-parallel east-west transects adapted from Chamberlain et al. (2018). Larose is a relatively landward site within the bayhead delta with thicker overbank deposits than at Galliano, a relatively seaward site. The reconstructed position of the mouth bar to overbank (M-O) boundary at the time of its formation is indicated by the dashed black line and the present-day position is indicated by the solid black line. OSL ages (black numbers) of mouth-bar deposits are given in ka relative to 2010 CE (see Chamberlain et al., 2018) and capture the time of M-O boundary formation. Boreholes excluded from the analysis (Table 1) are indicated by red tick marks.

0.3 m uncertainty (Hijma et al., 2015). All elevations are relative to NAVD 88. We calculate the subsidence rate (S) as:

$$S = \frac{\Delta E}{\Delta T}, \tag{2}$$

where ΔT is the difference between the time of formation of the M-O boundary (T_0, Figure 2c), obtained as the weighted mean of two mouth bar sand OSL ages for each site (Chamberlain et al., 2018) and 2010 CE (T_1, Figure 2c). We selected all Mississippi Delta sea-level index points (that is, datapoints with rigorously quantified uncertainties that capture the position of paleo-sea level in space and time; e.g., Engelhart et al., 2011) that formed during the time of Lafourche activity within 2σ uncertainty (Figure 2) from studies by González and Törnqvist (2009, $n = 28$) and Törnqvist et al. (2006, $n = 2$) to determine ΔRSL and express calibrated radiocarbon ages relative to 2010 CE for consistency with the OSL ages. A schematic synthesis of the method is shown in Figure 2c. Because ΔRSL is obtained from Mississippi Delta basal peat records, this term includes any deep subsidence due to processes with comparatively long wavelength, including glacial isostatic adjustment (GIA; Love et al., 2016) and sedimentary isostatic adjustment (SIA; Wolstencroft et al., 2014; Yu et al., 2012), but does not capture more localized deep subsidence due to faulting. In other words, the subtraction of ΔRSL removes broad-scale deep subsidence due to GIA and SIA while preserving any subsidence contribution due to faulting near our sites (Figure 3). Uncertainties are summed in quadrature. Cumulative values and rates of subsidence associated with the downward displacement of the M-O boundary are expressed as negative values.

2.2. Study Area and Stratigraphic Characterizations

We apply our new method to assess subsidence at 10 sites in the Lafourche subdelta of the Mississippi Delta (Figure 1; Table 1). The Lafourche distributary channel network is characterized by a single trunk channel landward of a "polyfurcation point" or bayhead delta apex and several smaller distributaries seaward of the polyfurcation point (Figure 1). Beginning at ~1.6 ka, the Lafourche subdelta prograded in a radial fashion from its apex to construct a 6,000–8,000 km^2 bayhead delta (Chamberlain et al., 2018). After ~1.2 ka, discharge was shared between the Lafourche and Modern (Balize) subdeltas and complete avulsion to the modern Mississippi River occurred ~0.6 ka (Hijma et al., 2017). The study sites are located along the banks of the bayhead delta's distributaries and their associated along-river distances are measured relative to the Lafourche-Modern avulsion site (Figure 1).

Each site hosts a transect of boreholes ($n = 64$) with depths ranging from 4.9 to 12.5 m that were hand-drilled and sampled between 2013 and 2015 CE (Chamberlain et al., 2018). We evaluated each borehole for suitability and rejected five boreholes where the M-O boundary was unclear or disturbed, often related to erosive paleochannels. We determined overbank deposit thickness between the land surface and the top of the mouth bar. We used the mean and standard deviation of all boreholes in a given transect to obtain average values for the depth of the M-O boundary and overbank deposit thickness at each site.

Three sites exhibit anthropogenic modification of the overbank deposits. The Dulac transect features an ~800 year old prehistoric earthen mound that appears to have enhanced subsidence of the underlying deposits (Chamberlain, Mehta, Reimann, & Wallinga, 2020), and the Cocodrie transect features ~20 cm of historic construction fill; no correction was made for this because the anthropogenic sediments were consolidated and have contributed to subsidence for decades to centuries. The Fourchon transect is in a region that has been actively elevated by dredge spoil pumping and features ~0.7–1.4 m of soft unconsolidated mud slurry overlying the overbank deposits at the time of coring; Google Earth imagery shows that the slurry was added within one year prior to our sampling. Here, we subtracted the unconsolidated anthropogenic mud from the overbank thickness because we deem it unlikely to have significantly contributed to subsidence.

Estimates of Holocene subsidence have been previously obtained for an inland site (Figure 1) within the Lafourche subdelta by measuring the displacement of a freshwater peat horizon formed at the coeval groundwater table (Törnqvist et al., 2008). We reanalyzed these data using a more recently published estimate of the local groundwater gradient (1 cm/km, González & Törnqvist, 2009), the tidal range obtained from NOAA tide gauges (tidesandcurrents.noaa.gov), and a ΔRSL reconstruction that matched our M-O boundary analysis. Törnqvist et al. (2008) identified a subset of their samples with low subsidence which they attributed to the presence of underlying sandy strata. We include this subset in our analysis; excluding it would not be justified because similar data are not available for the Lafourche bayhead delta deposits.

Oil and gas extraction (Morton et al., 2006) and faulting (Dokka et al., 2006; Kuecher et al., 2001) have also been identified as potential drivers of subsidence and thus implicated in Mississippi Delta land loss. We obtained oil and gas production data for our study area from the SONRIS database (http://www.sonris.com/) of the Louisiana Department of Natural Resources, and we took care to select study sites away from extraction hotspots when possible (Figure 1; see also Figures S1 and S2 in Supporting Information S1). We obtained Holocene succession thickness values (Figure 1) from Heinrich et al. (2015) to examine their relationship to subsidence. Whether listric growth faults, which are widespread across the Mississippi Delta (e.g., Fisk, 1944; McCulloh & Heinrich, 2012), have been sufficiently active throughout the late Holocene to drive extensive land loss in the Mississippi Delta is currently a subject of much debate (Dokka et al., 2006; Frederick et al., 2019; Shen et al., 2017). The Lafourche bayhead delta is crosscut by several fault zones and growth faults including the Golden Meadow and Lake Hatch faults (Gagliano et al., 2003; Kuecher et al., 2001); we consider their potential contributions to subsidence by comparing subsidence at locations landward and seaward of the faults (Figure 1).

2.3. Modeling Bayhead Delta Growth

Prior numerical model simulations of Mississippi Delta growth suggested that land building by means of sediment diversions is feasible (Kim, Mohrig, et al., 2009), although that model treated compaction as an instantaneous elevation drop when a delta prograded over bay mud. Here, we apply a modification of the

Journal of Geophysical Research: Earth Surface

10.1029/2021JF006153

Table 1
Stratigraphic, Geographic, and Chronologic Data, and Cumulative Values and Rates of Subsidence for the Cross Sections

Cross section	St. Charles	Raceland	Bayou Cane	Larose	Chauvin	Dulac	Cocodrie	Galliano	Golden Meadow	Fourchon	Paincourtville
Number of boreholes (total)	7	6	5	7	6	7	3	12	8	3	103
Number of boreholes (accepted)	6	6	3	7	6	7	3	10	8	3	103
Distance (river km)	64	82	75	106	106	103	130	127	132	165	17
Holocene succession thickness (m)	43	46	38	37	58	58	61	40	40	49	44
Overbank deposit thickness (m)	6.73 ± 1.31	5.92 ± 0.85	3.99 ± 0.85	4.20 ± 0.70	3.18 ± 1.13	6.63 ± 1.16	4.22 ± 0.25	1.66 ± 0.76	2.07 ± 0.70	0.46 ± 0.16	5.37 ± 2.17
E_1 (m, NAVD 88)	−4.32 ± 0.68	−4.09 ± 0.61	−3.10 ± 0.85	−3.10 ± 0.35	−3.23 ± 0.76	−5.45 ± 0.59	−3.53 ± 0.40	−2.15 ± 0.43	−2.48 ± 0.33	−0.73 ± 0.26	−2.33 ± 1.37
E_0 (m, NAVD 88)	−0.40 ± 0.20	−0.40 ± 0.20	−0.40 ± 0.20	−0.40 ± 0.20	−0.40 ± 0.20	−0.40 ± 0.20	−0.40 ± 0.20	−0.40 ± 0.20	−0.40 ± 0.20	−0.40 ± 0.20	0.45 ± 0.07
ΔT (ka)	1.49 ± 0.15	1.47 ± 0.11	1.46 ± 0.10	1.25 ± 0.08	1.10 ± 0.05	1.06 ± 0.05	0.94 ± 0.05	0.92 ± 0.07	0.92 ± 0.06	0.74 ± 0.06	1.42 ± 0.05
ΔRSL (m)	1.20 ± 0.30	1.18 ± 0.30	1.18 ± 0.30	1.05 ± 0.30	0.96 ± 0.30	0.94 ± 0.30	0.86 ± 0.30	0.85 ± 0.30	0.85 ± 0.30	0.75 ± 0.30	1.15 ± 0.30
Reconstructed elevation of boundary at formation time (m, NAVD 88)	−1.60 ± 0.36	−1.58 ± 0.36	−1.58 ± 0.36	−1.45 ± 0.36	−1.36 ± 0.36	−1.34 ± 0.36	−1.26 ± 0.36	−1.25 ± 0.36	−1.25 ± 0.36	−1.15 ± 0.36	−0.97 ± 0.31[a]
Cumulative subsidence, ΔE (m)	−2.73 ± 0.77	−2.51 ± 0.71	−1.53 ± 0.92	−1.65 ± 0.50	−1.88 ± 0.84	−4.11 ± 0.69	−2.27 ± 0.54	−0.89 ± 0.56	−1.22 ± 0.49	0.42 ± 0.44	−1.63 ± 1.40
Subsidence rate, S (mm/yr)	−1.83 ± 0.53	−1.71 ± 0.49	−1.04 ± 0.63	−1.31 ± 0.41	−1.71 ± 0.77	−3.88 ± 0.66	−2.41 ± 0.58	−0.97 ± 0.61	−1.34 ± 0.54	0.56 ± 0.60	−1.15 ± 0.99

Note. Chronologic data are from Chamberlain et al. (2018). Relative sea-level rise (ΔRSL) is determined using data from González and Törnqvist (2009) and Törnqvist et al. (2006). Holocene succession thickness data are from Heinrich et al. (2015). The other data presented here are novel to this study.

[a]Includes correction for groundwater table gradient.

Kim, Dai, et al. (2009) model informed by our field results to approximate compaction by the behavior of pressure-driven viscous fluids. We use this model because it captures delta shoreline progradation with time and constructs the break in slope between the delta topset and foreset (i.e., analogous to the M-O boundary) in a computationally efficient manner that is appropriate to the centennial to millennial timescales we investigate. The overlying topset thickness dictates pressure, and the gradient in the pressure determines the rate of compaction associated with the expulsion of pore water due to overburden loading. While we retain a background RSLR component of 0.5 mm/yr that includes the contributions of GIA, SIA, and geocentric sea-level rise (Figure 3) during the period of Lafourche activity, a key difference between our approach and that of Kim, Dai, et al. (2009) is that we do not use an instantaneous and spatially uniform compaction input. Rather, compaction in our updated model is a function of both time and space and happens in response to differential sediment loading. The model conserves mass yet allows the underlying mud substrate volume to change due to a simulated reduction in porosity. A compaction coefficient in the model is calibrated to match the observed relationship between overburden thickness (that is, the thickness of overbank deposits overlying the M-O boundary; see Supporting Information S1) and cumulative subsidence that we identify in the study area.

3. Results and Discussion

3.1. Subsidence Rates and Cumulative Values

We observe cumulative subsidence of up to −4.1 m (Table 1, Figure 5) and subsidence rates ranging from ∼0 to −4 mm/yr (Table 1, Figure S3 in Supporting Information S1). Additional subsidence likely occurs within the overbank deposits, which is not captured by our method. We note that cumulative subsidence for the Fourchon transect yielded a positive mean value that approaches zero within its uncertainty. This is interpreted not as exhumation but rather as a reflection of high uncertainty in our elevation estimate at this site due to anthropogenic alteration of the land surface through impoundment and dredge-spoil pumping. This datapoint can be read as little to no subsidence of the M-O boundary.

The load-driven component of subsidence has been previously shown to be greatest at the onset of loading and to decrease exponentially with time (e.g., Holtz & Kovacs, 1981), and the majority of compaction may occur within the first ∼20 year (Mazzotti et al., 2009). To investigate the time-dependent nature of the subsidence rates calculated here, we normalize rates by overburden thickness, yielding rates of subsidence (mm/yr) per meter of overbank sediment averaged over 750–1,500 years. These rates increase from older to younger sites (Figure 6). The age-wise trend in the normalized rates (i.e. higher normalized rates for younger deposits than for older deposits) indicates that load-induced subsidence is ongoing in the Lafourche subdelta, despite the passage of 750–1,500 years since loading began and about 600 years since loading ceased. Still, the present-day contributions of load-induced subsidence are likely very small compared to the average rate produced by our method.

Comparisons of such long-term rates can be valuable for assessing the processes active in delta-plain maintenance, especially if similar-timescale aggradation rates are also known (Chamberlain, Goodbred, Al Nahian, et al., 2020). In the Ganges-Brahmaputra Delta of Bangladesh, subsidence rates of about −2 to −4 mm/yr, also averaged over hundreds to thousands of years and obtained using the chronology of buried horizons, were determined by Grall et al. (2018) and attributed to buttressing of the delta by a thick succession of marine deposits. Our rates obtained for the Mississippi Delta are similar to those of Grall et al. (2018). However, we identify marine muds as a contributor to subsidence and interpret the relatively low (mm/yr) subsidence rates in both systems to simply be a function of averaging over a long timescale in relict portions of the deltas where load-induced compaction has slowed. Moreover, this comparison indicates that a similar sediment yield is needed to maintain the delta-plain area by offsetting RSLR in both deltas despite their vastly different tectonic settings. This has unfortunate implications for the sustainability of the Mississippi Delta, where sediment yield is about five times lower than in the Ganges-Brahmaputra Delta (Chamberlain, Goodbred, Hale, et al., 2020).

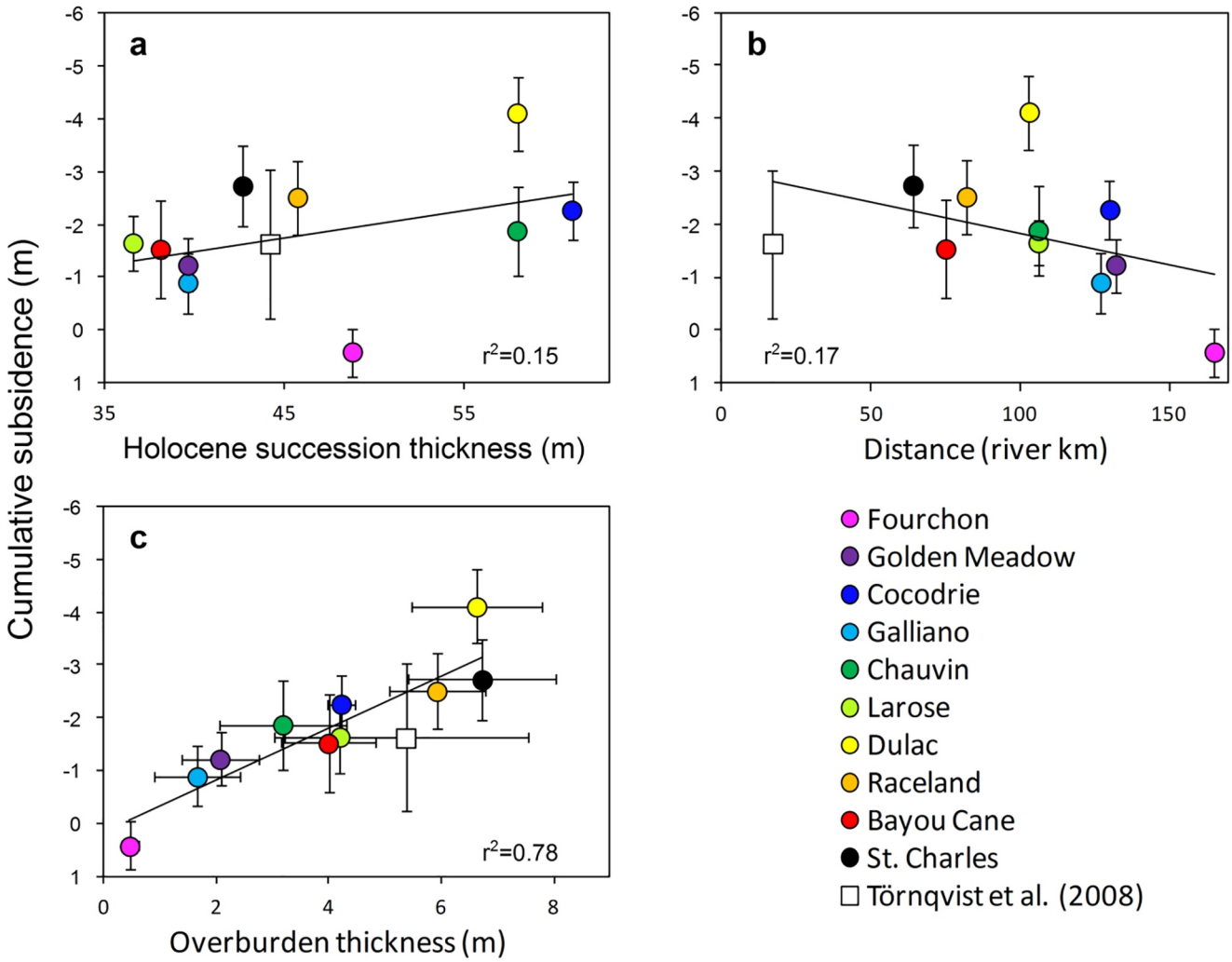

Figure 5. Mean cumulative subsidence at each site and its relationship to (a) The total local thickness of the Holocene succession, (b) Distance along Bayou Lafourche from the Lafourche-Modern avulsion site seaward, and (c) Overburden thickness. The cumulative subsidence values shown here are the average of all accepted boreholes at each site with uncertainties expressed as one standard deviation (see Supporting Information S1).

3.2. Stratigraphic, Tectonic, and Other Factors

The overbank unit is thickest at the bayhead delta apex and thins seaward (Figures 2a and 4) due to a shorter sedimentation time, that is, the time between the emergence of the mouth bar and the abandonment of the Lafourche subdelta at 0.6 ka (Chamberlain et al., 2018). Overbank deposits accumulated at an average rate of 0.7 cm/yr over the lifespan of the bayhead delta (Chamberlain, Mehta, Reimann, & Wallinga, 2020) and range in thickness from about 1–8 m at the sites studied herein (Table 1). These rates were determined from present-day (compacted) overbank-deposit thicknesses. Because the thickness of the mouth-bar and delta-front deposits is fairly uniform (Chamberlain et al., 2018), the thickness-trend of the overbank deposits yields a seaward-thinning, wedge-shaped geometry (Figure 2a). Cumulative subsidence is highest at the bayhead delta apex and lowest at the most seaward sites. Accommodation is therefore generated by subsidence near channels in proximal portions of the bayhead delta, a process that may inhibit superelevation and subsequent avulsion of the trunk channel (Liang et al., 2016). Our finding that spatial trends in subsidence may support trunk channel persistence is consistent with modeling of crevasse splays showing that the absence of subsidence results in channel choking (Nienhuis et al., 2018). This is consistent with the 1000-year growth history of the Lafourche bayhead delta which featured coactive distributary channels and no avulsions within the lobe (Chamberlain et al., 2018). The strong correlation of cumulative subsidence with

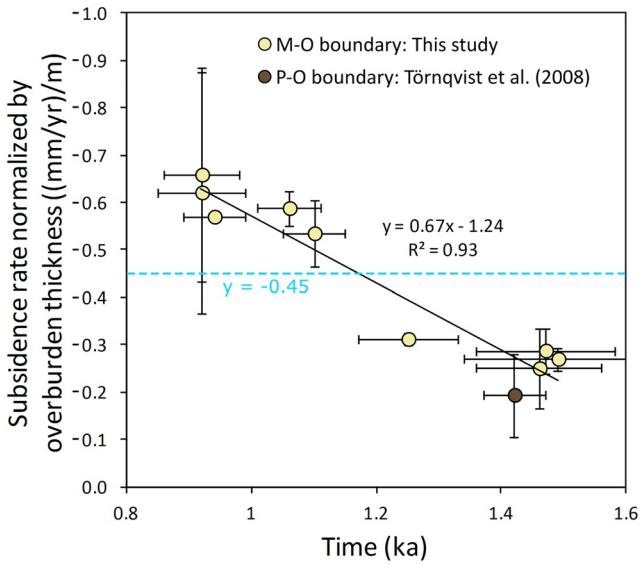

Figure 6. Subsidence rates normalized by overburden thickness are shown to decrease with time since formation of the mouth bar to overbank (M-O) and peat to overbank (P-O) boundaries. The blue dashed line indicates the average normalized subsidence rate of the M-O boundary. The Fourchon cross-section was excluded from this analysis because it produced outlying values likely related to uncertainty in the land surface elevation due to anthropogenic modification. The vertical uncertainty on some points is very small, indicated by a lack of visible error bars.

overburden thickness (Figures 5c and 7) supports previous findings that compaction due to sediment loading is a primary driver of subsidence in actively aggrading deltas (e.g., Törnqvist et al., 2008) although rates of compaction-driven subsidence slow down and become less important after loading ceases.

We find no relationship between subsidence and the total thickness of the Holocene succession at our study sites (r^2 = 0.15, Figure 5a). Comparisons with other deltas also do not show a clear connection; our rates for the Mississippi Delta are similar to those documented in the Ganges-Brahmaputra Delta (Grall et al., 2018) despite its significantly thicker Holocene sediment package (up to 90 m; Goodbred & Kuehl, 1999) yet lower than millennial-timescale estimates of about −17 mm/yr for the progradational portion of the Mekong Delta where Holocene sediment thicknesses are only ~18–25 m (Zoccarato et al., 2018). Collectively, this evidence highlights the fact that a large proportion of sediment compaction occurs in the shallowest subsurface (e.g., <5 m; Keogh & Törnqvist, 2019).

We also see little impact from oil and gas extraction–the surface expression of which corresponds to the depth of wells such that deeper wells possess a greater footprint. The deepest wells and greatest extraction values are generally found at seaward locations in our study area (e.g., Golden Meadow and Fourchon sites; Figure 1; Figures S1 and S2 in Supporting Information S1) where subsidence values obtained with our method are the lowest. This can be attributed in part to our selection of study sites away from oil and gas fields. Over the spatial and temporal scales we studied, the total thickness of the entire Holocene succession also appears to be of little importance although it remains a significant factor in basin-wide subsidence trends acting over longer (i.e., >10^4 yr) timescales (Frederick et al., 2019) and measured at greater depths (Karegar et al., 2015). These seemingly contradictory observations can be reconciled by taking account of the fact that compaction rates increase both with reduced accumulation time of a given deposit thickness, but also with an increase in total deposit thickness for a given accumulation time (Meckel et al., 2006, 2007). In other words, compaction rates are governed by complex physical processes that can yield apparently disparate field results when measured over different depth and time scales.

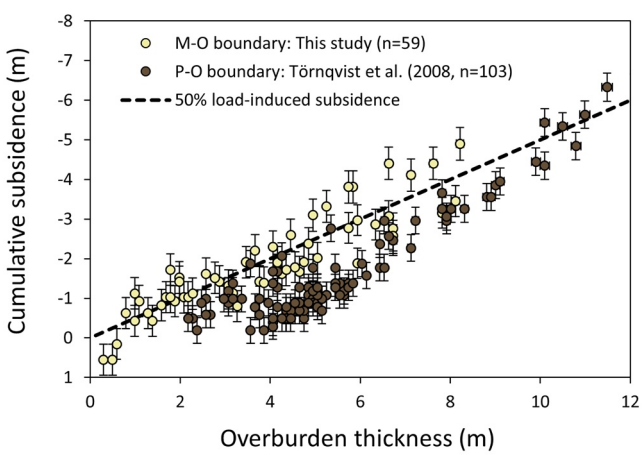

Figure 7. The relationship of overburden thickness to cumulative subsidence assessed with two indicators: the mouth bar to overbank (M-O) boundary (this study) and the peat to overbank (P-O) boundary (Törnqvist et al., 2008). The dashed line indicates cumulative subsidence equivalent to 50% of the overburden thickness. The data shown here represent individual boreholes rather than the site averages shown in Figure 5c.

Some studies have claimed that fault movement in the Mississippi Delta has driven a general trend of seaward increasing subsidence, associated with the submergence of large blocks of coastal land (Dokka et al., 2006; Gagliano et al., 2003). We find no evidence for such a trend (r^2 = 0.17, Figure 5b) in the shallow-subsidence data that we collected and no enhanced subsidence is observed seaward of previously mapped faults. For example, the rate of subsidence of the Golden Meadow transect (−1.34 ± 0.54 mm/yr) located seaward of the Golden Meadow Fault (Kuecher et al., 2001) is not significantly different from the rate of subsidence at the Galliano transect (−0.97 ± 0.61 mm/yr) located landward of this fault. Similarly, the subsidence rate of the Larose transect located seaward of the Lake Hatch Fault (−1.31 ± 0.41 mm/yr) is lower than that of the Raceland transect located landward of this fault (−1.71 ± 0.49 mm/yr). Despite uncertainty in the exact surface expression of faults in our study area, the lack of a seaward increase of subsidence suggests that faulting is producing at most only limited, local effects in the Mississippi Delta (e.g., Hopkins et al., 2021) and is not

driving broad-scale subsidence in this part of the delta, consistent with the slow long-term rates of fault slip inferred by Frederick et al. (2019).

3.3. Paleoenvironmental Factors

The prevalence of subsurface peat is commonly linked to the highest rates of subsidence, indicating that organic-rich, terrestrial environments may be more compaction-prone than dominantly clastic estuarine bays. Törnqvist et al. (2008) estimated that 35% of elevation gained by overbank deposition is lost to shallow subsidence at an inland site in the Mississippi Delta underlain by peat (Figure 1); we obtain the value of 28% mainly due to the inclusion of the data excluded by Törnqvist et al. (2008). By reconstructing the original position of the M-O boundary at the time of its formation (Figure 4) and calculating the fraction of the overlying deposit occurring below this boundary at present-day, we estimate that ~50% of elevation gained by the bayhead delta through overbank deposition is ultimately lost to subsidence (Figure 7). Our value is considerably higher than the 28%–35% value for load-induced subsidence at more inland localities underlain by peat (Törnqvist et al., 2008). This indicates that estuarine bays are especially prone to subsidence driven by load-induced compaction, consistent with observations of high subsidence rates associated with muddy Holocene strata elsewhere (e.g., Higgins et al., 2014; Zoccarato et al., 2018). The high vulnerability of muds to subsidence may be due to dewatering of deltaic sediments. The alternating layers of sand and clay typical of bayhead delta stratigraphy may generate optimal conditions for compaction because the high permeability of sand allows groundwater to escape, lowering the porewater overpressure (Meckel et al., 2006). By contrast, peats confined by low-permeability clays—a condition typical of settings farther inland, upstream of the bayhead delta—are less likely to expel groundwater and may therefore be less prone to compaction.

3.4. Modeling Delta Growth Under a Data-Driven Compaction Scenario

Our findings imply that inactive portions of the delta plain may be fairly stable if they are not loaded. However, this is an unlikely condition in many deltas and especially in the Mississippi Delta where proposed delta restoration strategies may introduce large quantities of new sediment onto compaction-prone bay strata. To test whether load-driven subsidence by engineered diversions may significantly inhibit their land-building efficacy, we employed a modified version of the delta-growth model of Kim, Dai, et al. (2009) informed by our findings (Figure 8). We approximated sediment discharge based on the dimensions of Lafourche delta deposits along with an opening angle of 70° (Figure 1) and a basement with a slope of -4×10^{-5} based on the field measurements (Figure 8d). We first ran the model with the initially sloped basement and a range of water discharges to match the Lafourche bayhead delta topset slope of 4×10^{-5} (a 4 m rise over a ~100 km run) observed in the field data (Figure 8d). The model organized a topset slope of 4.01×10^{-5} at a flood discharge of 10,240 m^3/s. RSLR was set at 0.5 mm/yr and the deposit porosity was assumed at 0.6 (an average value of initial bar sand, bay mud, and prodelta deposits before compaction; Kuecher, 1994; Meckel et al., 2007). The model produced a shoreline advance of 108.8 km over 1,000 years under these conditions (Figure 8a), which is matched with ~100 km progradation observed in the Lafourche bayhead delta. We then applied the same parameters to the tuned model to examine two scenarios: one with compaction scaled to 50% of the delta topset (i.e., overburden thickness), and one with no compaction, both over an initially flat basement at −4 m depth. These parameters approximate the growth conditions of the Lafourche bayhead delta. A detailed description of the model and its compaction component is provided in Supporting Information S1.

Under conditions with compaction, the delta prograded ~110 km to build ~7,800 km^2 of new deltaic land and the land-surface elevation at the delta apex gained up to ~4.2 m of elevation (Figure 8b). With no compaction, the delta shoreline prograded ~10 km farther to build an additional ~1,100 km^2 of land and gained ~0.7 m of additional elevation at the delta apex (Figure 8c) compared to the results from the compaction case. Both scenarios closely reproduce the Lafourche bayhead delta planform growth, suggesting the model is valid for our aims, although we note that modeled delta progradation rates slow with time whereas a constant, linear rate of progradation was documented for the Lafourche subdelta (Chamberlain et al., 2018). Chamberlain et al. (2018) hypothesized that other mechanisms such as enhanced mud retention in the interdistributary basins of maturing deltas may sustain progradation rates by filling the incrementally greater space between distributaries associated with the widening planform with time. Said differently, a constant

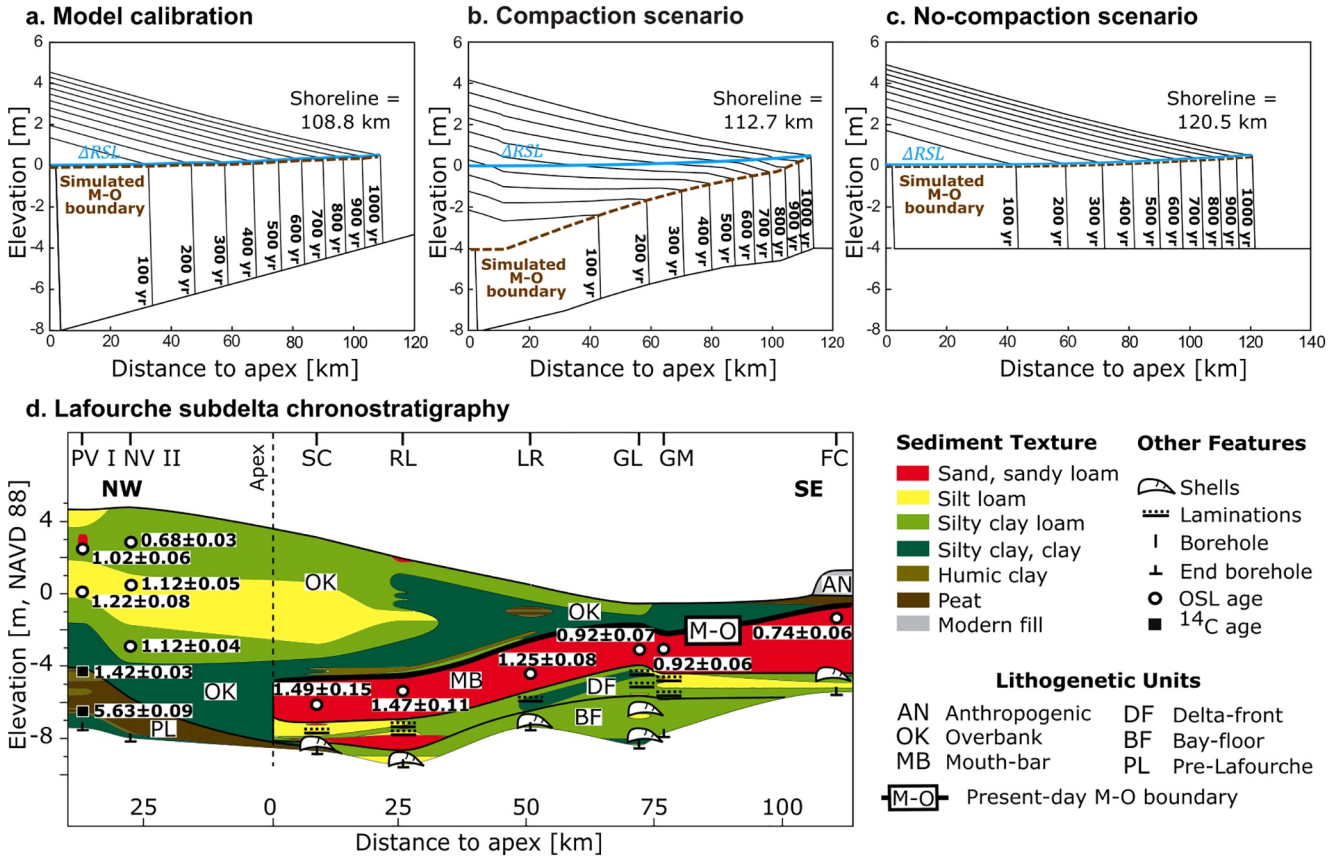

Figure 8. Numerical modeling of bayhead delta progradation under scenarios with (a) An initially sloped basement for purposes of determining the input parameters, for example, sediment supply and water discharge, (b) An initially flat basement and compaction scaled to 50% overburden thickness and (c) An initially flat basement and no compaction. (d) Dip-oriented Lafourche subdelta chronostratigraphy adapted from Chamberlain et al. (2018) for comparison. The modeled scenarios show similar total shoreline progradation to the field data and one another, suggesting the model is valid and compaction has a limited impact on delta progradation. The (post-compaction) depth of the simulated mouth bar to overbank (M-O) boundary is indicated by the brown dashed line. In the compaction scenario (b), the M-O boundary is located at about −4 m at the bayhead-delta apex and shallows seaward with decreasing overburden, similar to the stratigraphy identified in the Lafourche bayhead delta.

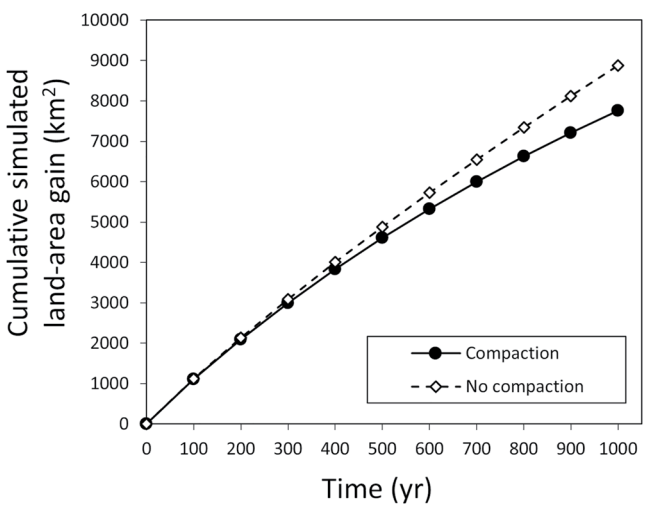

Figure 9. Cumulative simulated land-area gain as a function of time for each 100 year time step, for the model scenarios with (Figure 8b) and without compaction (Figure 8c).

progradation rate would require an increase in land-area gain with time due to the widening of the delta's planform. Sand can generally be considered the limiting factor in Mississippi Delta growth; sand forms the mouth bar framework that facilitates progradation (Chamberlain et al., 2018) yet sand comprises <30% of the annual sediment load to the delta while mud comprises the majority (Allison et al., 2012). Mature deltas may serve as more efficient mud traps, thereby promoting increased rates of land-area gain coupled with sustained progradation rates. Alternatively, discrepancies between the model and the Lafourche bayhead delta may be due to temporal variation in sediment discharge which is presently unknown.

Delta progradation under the modeled compaction scenario is reduced by ~6%, and the surface-area gain is reduced by ~13% over the 1,000 year of simulation (Figure 9, Table S1 in Supporting Information S1). After the first 100 years of simulation (a typical engineering timescale), delta progradation under the compaction scenario is only reduced by ~0.4% and the surface-area gain is reduced by ~0.7% (Figure 9, Table S1 in Supporting Information S1). We caution against overinterpreting the results of the first hundred years of model simulation because our model is less

suited for projecting delta growth over short timescales than other, more sophisticated morphodynamic models (e.g., Delft3D).

Both the Lafourche bayhead delta and the model deltas have a fan shape in planform. In the compaction model scenario, the greatest vertical displacement of the M-O boundary occurs near the delta apex covering a relatively small area, which results in a small overall loss of deposit volume due to compaction. Displacement of the simulated M-O boundary shallows seaward with decreasing overburden, similar to the stratigraphy identified in the Lafourche subdelta (Figure 8d). A greater volume of sediment is deposited over the much wider downstream portion of the fan-shaped delta. This downstream section is the relatively thin and newly prograded part of the delta, so the compaction effect is much smaller. Lateral migration of the apex channel can deposit a greater volume of sediment closer to the delta apex than the downstream portion and cause significant loss of elevation by compaction. On the other hand, the enhanced compaction at the delta apex promotes the maintenance of distributary channels that feed growth of the delta (Liang et al., 2016). In sum, our model results indicate that delta progradation and associated deltaic land-area gain can be sustained even under a realistic compaction scenario. Furthermore, load-driven compaction may in fact promote the viability of emergent coastal landforms including engineered diversions by sustaining the feeder channel. Similar to a recent model study that examined crevasse-splay formation in relation to shallow subsidence (Nienhuis et al., 2018), we find that sediment compaction is not necessarily a detrimental process with respect to land building in deltas.

Finally, the new findings presented here are also relevant to sequence-stratigraphic analyses of deltaic successions in deeper time, most notably trajectory analysis that is widely used in the rock record. Our case study from the Mississippi Delta offers an exceptionally highly resolved example of an ascending regressive shoreline trajectory with an observed angle of about 0.0023°, which is at the low end of the range of such angles synthesized by Helland-Hansen and Hampson (2009). Nevertheless, we note that this angle would have been even eight times lower (0.0003°, i.e., essentially flat) in the absence of sediment compaction (i.e., Figures 8b vs. 8c). In other words, in mud-rich deltaic systems, sediment compaction can play a substantial role in affecting the shoreline trajectory and the associated thickness of facies belts, something that deserves consideration in the interpretation of the ancient rock record.

4. Conclusions

We present a new method for quantifying local RSLR in river-dominated deltas and use our findings to assess the role of subsidence in delta growth. Our method makes use of a stratigraphic boundary that is common to river-dominated deltas and other coastal systems. Combined with recent advancements in sediment dating (i.e., OSL), this offers a means to test centennial-to millennial-timescale subsidence rates in deltas, a key element in assessing sustainability and management strategies for these vital landscapes. Applying this method to the Mississippi Delta, we arrive at the following conclusions:

1. Load-induced subsidence of shallow strata is a primary component of deltaic subsidence, while deeper processes such as faulting, oil and gas extraction, and compaction of the entire Holocene sediment package appear to have little impact over the space and time scales and at the locations we consider.
2. Mud-dominated bayfloor deposits may experience greater shallow subsidence than peat beds; up to 50% of elevation gained by overbank deposition in a growing delta may be lost to shallow subsidence
3. Sediment loading and load-driven compaction are greatest at the delta apex, promoting the maintenance of a stable trunk channel and enabling continued sedimentation; these processes diminish radially downstream and have only a minor effect on progradation of the delta front
4. Despite rapid shallow subsidence during bayhead delta progradation, sediment compaction has a limited effect on the rate and magnitude of land building

In sum, this work provides new insights into how shallow subsidence operates in deltas and yields the surprising finding that bay-floor muds may be more compaction-prone than peats. Nevertheless, the high vulnerability to compaction of prograding deltas has a limited effect on the growth that can be accomplished through engineered sediment diversions.

Data Availability Statement

Data sets for this research are included in this article and its Supporting Information S1. Supporting stratigraphic details and subsidence calculations for each borehole are publicly accessible in the 4TU. Reaserch Data online repository at https://doi.org/10.4121/14170919.v2. Louisiana oil and gas production data are available online through the SONRIS database (http://www.sonris.com/) of the Louisiana Department of Natural Resources.

Acknowledgments
This work was supported by grants from the Coastal Protection and Restoration Authority of the Louisiana Applied Research Program (CPRA-2013-T11-SBO2-DR) and the Gulf Coast Association of Geological Societies student grant program, with additional support from the U.S. National Science Foundation (EAR-1148005, EAR-1148247, and EAR-1349311). Contributions of W. Kim were supported in part by the Basic Science Research Program through the National Research Foundation of Korea (NRF-2020R1A2C1006083 and NRF-2017R1A6A1A07015374), and E. L. Chamberlain was supported by a postdoctoral award from the U.S. National Science Foundation (EAR-1855264) during manuscript synthesis. The authors thank J. Bridgeman, C. Esposito, and J. Mehta for field assistance, M. Hopkins and J. Shaw for helpful conversations, and M.A. Allison, S.L. Goodbred, R. Sincavage, and J. Wallinga for comments on an earlier draft. This work benefited from feedback provided by a coastal neotectonics and subsidence expert panel, notably from J.B. Anderson, and from reviews by P. Teatini, A. Moodie, and an anonymous reviewer. This is a contribution to the PALSEA program.

References

Allison, M., Yuill, B., Törnqvist, T., Amelung, F., Dixon, T. H., Erkens, G., et al. (2016). Global risks and research priorities for coastal subsidence. *Eos*, *97*(19), 22–27. https://doi.org/10.1029/2016eo055013

Allison, M. A., Demas, C. R., Ebersole, B. A., Kleiss, B. A., Little, C. D., Meselhe, E. A., et al. (2012). A water and sediment budget for the lower Mississippi-Atchafalaya River in flood years 2008–2010: Implications for sediment discharge to the oceans and coastal restoration in Louisiana. *Journal of Hydrology*, *432–433*, 84–97. https://doi.org/10.1016/j.jhydrol.2012.02.020

Bijlsma, L., Ehler, C., Klein, R., Kulshrestha, S., McLean, R., Mimura, N., et al. (1996). *Coastal zones and small islands* (pp. 289–324). Cambridge University Press.

Brivio, L., Ghinassi, M., D'Alpaos, A., Finotello, A., Fontana, A., Roner, M., & Howes, N. (2016). Aggradation and lateral migration shaping geometry of a tidal point bar: An example from salt marshes of the Northern Venice Lagoon (Italy). *Sedimentary Geology*, *343*, 141–155. https://doi.org/10.1016/j.sedgeo.2016.08.005

Cahoon, D. R., Reed, D. J., & Day, J. W., Jr. (1995). Estimating shallow subsidence in microtidal salt marshes of the southeastern United States: Kaye and Barghoorn revisited. *Marine Geology*, *128*(1–2), 1–9. https://doi.org/10.1016/0025-3227(95)00087-f

Chamberlain, E. L., Goodbred, S. L., Al Nahian, A., Rahman, F. A., Reimann, T., Steckler, M. S., et al. (2020). Competition between little channels and big earthquakes to drive river avulsion timescales. Paper presented at the AGU Fall Meeting 2020.

Chamberlain, E. L., Goodbred, S. L., Hale, R., Steckler, M. S., Wallinga, J., & Wilson, C. (2020). Integrating geochronologic and instrumental approaches across the Bengal Basin. *Earth Surface Processes and Landforms*, *45*(1), 56–74. https://doi.org/10.1002/esp.4687

Chamberlain, E. L., Mehta, J. M., Reimann, T., & Wallinga, J. (2020). A geoarchaeological perspective on the challenges and trajectories of Mississippi Delta communities. *Geomorphology*. https://doi.org/10.1016/j.geomorph.2020.107132

Chamberlain, E. L., Törnqvist, T. E., Shen, Z., Mauz, B., & Wallinga, J. (2018). Anatomy of Mississippi Delta growth and its implications for coastal restoration. *Science Advances*, *4*(4), eaar4740. https://doi.org/10.1126/sciadv.aar4740

Couvillion, B. R., Beck, H. J., Schoolmaster, D., & Fischer, M. (2017). *Land area change in coastal Louisiana (1932–2016)*.

CPRA. (2017). *Louisiana's comprehensive master plan for a susutainable coast*. Coastal Protection and Restoration Authority of Louisiana.

Cunningham, R., Gisclair, D., & Craig, J. (2004). *The Louisiana statewide lidar project*. Retrieved from ftp://ftp-fc.sc.egov.usda.gov/NCGC/products/elevation/la-lidar-project.pdf

Dokka, R. K., Sella, G. F., & Dixon, T. H. (2006). Tectonic control of subsidence and southward displacement of southeast Louisiana with respect to stable North America. *Geophysical Research Letters*, *33*, L23308. https://doi.org/10.1029/2006gl027250

Edmonds, D. & Slingerland, R. (2007). Mechanics of river mouth bar formation: Implications for the morphodynamics of delta distributary networks. *Journal of Geophysical Research*, *112*(F2). https://doi.org/10.1029/2006jf000574

Engelhart, S. E., Horton, B. P., & Kemp, A. C. (2011). Holocene sea level changes along the United States' Atlantic Coast. *Oceanography*, *24*(2), 70–79. https://doi.org/10.5670/oceanog.2011.28

Ericson, J. P., Vörösmarty, C. J., Dingman, S. L., Ward, L. G., & Meybeck, M. (2006). Effective sea-level rise and deltas: Causes of change and human dimension implications. *Global and Planetary Change*, *50*(1–2), 63–82. https://doi.org/10.1016/j.gloplacha.2005.07.004

Fisk, H. N. (1944). *Geological investigation of the Alluvial valley of the lower Mississippi River*. Vicksburg.

Fisk, H. N., McFarlan, E., Jr., Kolb, C. R., & Wilbert, L. J., Jr. (1954). Sedimentary framework of the modern Mississippi delta. *Journal of Sedimentary Petrology*, *24*, 76–99. https://doi.org/10.1306/d4269661-2b26-11d7-8648000102c1865d

Frederick, B. C., Blum, M., Fillon, R., & Roberts, H. (2019). Resolving the contributing factors to Mississippi Delta subsidence: Past and Present. *Basin Research*, *31*(1), 171–190. https://doi.org/10.1111/bre.12314

Gagliano, S. M., Kemp, E. B., III, Wicker, K. M., Wiltenmuth, K. S., & Sabate, R. W. (2003). Neo-tectonic framework of southeast Louisiana and applications to coastal restoration. *GCAGS Transactions*, *53*, 262–276.

Gesch, D. B. (2018). Best practices for elevation-based assessments of sea-level rise and coastal flooding exposure. *Frontiers in Earth Science*, *6*, 230. https://doi.org/10.3389/feart.2018.00230

González, J. L., & Törnqvist, T. E. (2009). A new late Holocene sea-level record from the Mississippi Delta: Evidence for a climate/sea level connection? *Quaternary Science Reviews*, *28*(17–18), 1737–1749. https://doi.org/10.1016/j.quascirev.2009.04.003

Goodbred, S. L., & Kuehl, S. A. (1999). Holocene and modern sediment budgets for the Ganges-Brahmaputra river system: Evidence for highstand dispersal to flood-plain, shelf, and deep-sea depocenters. *Geology*, *27*, 559–562. https://doi.org/10.1130/0091-7613(1999)027<0559:hamsbf>2.3.co;2

Grall, C., Steckler, M., Pickering, J., Goodbred, S., Sincavage, R., Paola, C., et al. (2018). A base-level stratigraphic approach to determining Holocene subsidence of the Ganges-Meghna-Brahmaputra Delta plain. *Earth and Planetary Science Letters*, *499*, 23–36. https://doi.org/10.1016/j.epsl.2018.07.008

Heinrich, P., Paulsell, R., Milner, R., Snead, J., & Peele, H. (2015). *Investigation and GIS development of the buried Holocene-Pleistocene surface in the Louisiana coastal plain*. Louisiana State University, Louisiana Geological Survey.

Helland-Hansen, W., & Hampson, G. (2009). Trajectory analysis: Concepts and applications. *Basin Research*, *21*(5), 454–483.

Higgins, S. A. (2016). Advances in delta-subsidence research using satellite methods. *Hydrogeology Journal*, *24*(3), 587–600. https://doi.org/10.1007/s10040-015-1330-6

Higgins, S. A., Overeem, I., Steckler, M. S., Syvitski, J. P., Seeber, L., & Akhter, S. H. (2014). InSAR measurements of compaction and subsidence in the Ganges-Brahmaputra Delta, Bangladesh. *Journal of Geophysical Research: Earth Surface*, *119*(8), 1768–1781. https://doi.org/10.1002/2014jf003117

Hijma, M. P., Engelhart, S. E., Törnqvist, T. E., Horton, B. P., Hu, P., & Hill, D. F. (2015). A protocol for a geological sea-level database. In I. Shennan, A. J. Long, & B. P. Horton (Eds.), *Handbook of sea-level research* (pp. 536–553). Wiley Blackwell. https://doi.org/10.1002/9781118452547.ch34

Hijma, M. P., Shen, Z., Törnqvist, T. E., & Mauz, B. (2017). Late Holocene evolution of a coupled, mud-dominated delta plain-chenier plain system, coastal Louisiana, USA. *Earth Surface Dynamics*, *5*(4), 689–710. https://doi.org/10.5194/esurf-5-689-2017

Hill, D. F., Griffiths, S. D., Peltier, W. R., Horton, B. P., & Törnqvist, T. E. (2011). High-resolution numerical modeling of tides in the western Atlantic, Gulf of Mexico, and Caribbean Sea during the Holocene. *Journal of Geophysical Research*, *116*, C10014. https://doi.org/10.1029/2010jc006896

Holtz, R. D., & Kovacs, W. D. (1981). *An introduction to geotechnical engineering*. Prentice-Hall.

Hopkins, M. C., Lopez, J., & Songy, A. (2021). Coastal subsidence due to faults: Insights from elevation profiles of vehicular bridges, southeastern Louisiana, USA. *Journal of Coastal Research*. https://doi.org/10.2112/JCOASTRES-D-21-00015.1

Jankowski, K. L., Törnqvist, T. E., & Fernandes, A. M. (2017). Vulnerability of Louisiana's coastal wetlands to present-day rates of relative sea-level rise. *Nature Communications*, *8*, 14792. https://doi.org/10.1038/ncomms14792

Jelgersma, S. (1996). Land subsidence in coastal lowlands. In *Sea-level rise and coastal subsidence* (pp. 47–62). Springer. https://doi.org/10.1007/978-94-015-8719-8_3

Karegar, M. A., Dixon, T. H., & Malservisi, R. (2015). A three-dimensional surface velocity field for the Mississippi Delta: Implications for coastal restoration and flood potential. *Geology*, *43*(6), 519–522. https://doi.org/10.1130/g36598.1

Kaye, C. A., & Barghoorn, E. S. (1964). Late Quaternary sea-level change and crustal rise at Boston, Massachusetts, with notes on the autocompaction of peat. *Geological Society of America Bulletin*, *75*(2), 63–80. https://doi.org/10.1130/0016-7606(1964)75[63:lqscac]2.0.co;2

Keogh, M. E., & Törnqvist, T. E. (2019). Measuring rates of present-day relative sea-level rise in low-elevation coastal zones: A critical evaluation. *Ocean Science*, *15*(1), 61–73. https://doi.org/10.5194/os-15-61-2019

Kim, W., Dai, A., Muto, T., & Parker, G. (2009). Delta progradation driven by an advancing sediment source: Coupled theory and experiment describing the evolution of elongated deltas. *Water Resources Research*, *45*(6). https://doi.org/10.1029/2008wr007382

Kim, W., Mohrig, D., Twilley, R., Paola, C., & Parker, G. (2009). Is it feasible to build new land in the Mississippi River delta? *Eos, Transactions American Geophysical Union*, *90*, 373–374. https://doi.org/10.1029/2009eo420001

Kolker, A. S., Allison, M. A., & Hameed, S. (2011). An evaluation of subsidence rates and sea-level variability in the northern Gulf of Mexico. *Geophysical Research Letters*, *38*, L21404. https://doi.org/10.1029/2011gl049458

Kuecher, G., Roberts, H., Thompson, M., & Matthews, I. (2001). Evidence for active growth faulting in the Terrebonne delta plain, south Louisiana: Implications for wetland loss and the vertical migration of petroleum. *Environmental Geosciences*, *8*(2), 77–94. https://doi.org/10.1046/j.1526-0984.2001.82001.x

Kuecher, G. J. (1994). *Geologic framework and consolidation settlement potential of the Lafourche delta, Topstratum valley fill; Implications for Wetland Loss in Terrebonne and Lafourche Parishes*. Louisiana.

Liang, M., Kim, W., & Passalacqua, P. (2016). How much subsidence is enough to change the morphology of river deltas? *Geophysical Research Letters*, *43*(19), 10266–10276. https://doi.org/10.1002/2016gl070519

Love, R., Milne, G. A., Tarasov, L., Engelhart, S. E., Hijma, M. P., Latychev, K., et al. (2016). The contribution of glacial isostatic adjustment to projections of sea-level change along the Atlantic and Gulf coasts of North America. *Earth's Future*, *4*(10), 440–464. https://doi.org/10.1002/2016ef000363

Mazzotti, S., Lambert, A., Van der Kooij, M., & Mainville, A. (2009). Impact of anthropogenic subsidence on relative sea-level rise in the Fraser River delta. *Geology*, *37*(9), 771–774. https://doi.org/10.1130/g25640a.1

McCulloh, R. P., & Heinrich, P. V. (2012). Surface faults of the south Louisiana growth-fault province. In *Recent Advances in North American Paleoseismology and Neotectonics East of the Rockies* (Vol. *493*, pp. 37–51). Geological Society of America, Special Papers.

Meckel, T. A., Ten Brink, U. S., & Williams, S. J. (2006). Current subsidence rates due to compaction of Holocene sediments in southern Louisiana. *Geophysical Research Letters*, *33*, L11403. https://doi.org/10.1029/2006gl026300

Meckel, T. A., Ten Brink, U. S., & Williams, S. J. (2007). Sediment compaction rates and subsidence in deltaic plains: Numerical constraints and stratigraphic influences. *Basin Research*, *19*, 19–31. https://doi.org/10.1111/j.1365-2117.2006.00310.x

Milliman, J., & Haq, B. U. (1996). *Sea-level rise and coastal subsidence. Causes, consequences, and strategies* (Vol. *2*). Kluwer.

Morton, R. A., Bernier, J. C., & Barras, J. A. (2006). Evidence of regional subsidence and associated interior wetland loss induced by hydrocarbon production, Gulf Coast region, USA. *Environmental Geology*, *50*, 261–274. https://doi.org/10.1007/s00254-006-0207-3

Nienhuis, J., Ashton, A., Edmonds, D., Hoitink, A., Kettner, A., Rowland, J., & Törnqvist, T. (2020). Global-scale human impact on delta morphology has led to net land area gain. *Nature*, *577*(7791), 514–518. https://doi.org/10.1038/s41586-019-1905-9

Nienhuis, J. H., Törnqvist, T. E., & Esposito, C. R. (2018). Crevasse splays vs. avulsions: A recipe for land building with levee breaches. *Geophysical Research Letters*, *45*(9), 4058–4067. https://doi.org/10.1029/2018gl077933

Olliver, E. A., & Edmonds, D. A. (2017). Defining the ecogeomorphic succession of land building for freshwater, intertidal wetlands in Wax Lake Delta, Louisiana. *Estuarine, Coastal and Shelf Science*, *196*, 45–57. https://doi.org/10.1016/j.ecss.2017.06.009

Paola, C., Twilley, R. R., Edmonds, D. A., Kim, W., Mohrig, D., Parker, G., et al. (2011). Natural processes in delta restoration: Application to the Mississippi Delta. *Annual Review of Marine Science*, *3*(3), 67–91. https://doi.org/10.1146/annurev-marine-120709-142856

Roberts, H. H., Walker, N., Cunningham, R., Kemp, G. P., & Majersky, S. (1997). Evolution of sedimentary architecture and surface morphology: Atchafalaya and Wax Lake deltas, Louisiana (1973–1994). *Gulf Coast Association of Geological Societies Transactions*, *47*, 477–484.

Shen, Z., Dawers, N. H., Törnqvist, T. E., Gasparini, N. M., Hijma, M. P., & Mauz, B. (2017). Mechanisms of late Quaternary fault throw-rate variability along the north central Gulf of Mexico coast: Implications for coastal subsidence. *Basin Research*, *29*(5), 557–570. https://doi.org/10.1111/bre.12184

Shen, Z. X., & Mauz, B. (2012). Optical dating of young deltaic deposits on a decadal time scale. *Quaternary Geochronology*, *10*, 110–116. https://doi.org/10.1016/j.quageo.2012.01.014

Shirzaei, M., Freymueller, J., Törnqvist, T. E., Galloway, D. L., Dura, T., & Minderhoud, P. S. (2021). Measuring, modeling and projecting coastal land subsidence. *Nature Reviews Earth & Environment*, *2*, 40–58. https://doi.org/10.1038/s43017-020-00115-x

Steyer, G. D., Sasser, C. E., Visser, J. M., Swenson, E. M., Nyman, J. A., & Raynie, R. C. (2003). A proposed coast-wide reference monitoring system for evaluating wetland restoration trajectories in Louisiana. In B. D. Melzian, V. Engle, M. McAlister, S. Sandhu, & L. K. Eads (Eds.), *Coastal monitoring through partnerships*. Springer. https://doi.org/10.1007/978-94-017-0299-7_11

Syvitski, J. P. M., Vörösmarty, C. J., Kettner, A. J., & Green, P. (2005). Impact of humans on the flux of terrestrial sediment to the global coastal ocean. *Science*, *308*, 376–380. https://doi.org/10.1126/science.1109454

Teatini, P., Tosi, L., & Strozzi, T. (2011). Quantitative evidence that compaction of Holocene sediments drives the present land subsidence of the Po Delta, Italy. *Journal of Geophysical Research*, *116*(B8). https://doi.org/10.1029/2010jb008122

Törnqvist, T. E., Bick, S. J., van der Borg, K., & de Jong, A. F. (2006). How stable is the Mississippi Delta? *Geology*, *34*(8), 697–700.

Törnqvist, T. E., Wallace, D. J., Storms, J. E. A., Wallinga, J., Van Dam, R. L., Blaauw, M., et al. (2008). Mississippi Delta subsidence primarily caused by compaction of Holocene strata. *Nature Geoscience*, *1*(3), 173–176. https://doi.org/10.1038/ngeo129

Van Asselen, S., Stouthamer, E., & Van Asch, T. W. J. (2009). Effects of peat compaction on delta evolution: A review on processes, responses, measuring and modeling. *Earth-Science Reviews*, *92*(1–2), 35–51. https://doi.org/10.1016/j.earscirev.2008.11.001

Webb, E. L., Friess, D. A., Krauss, K. W., Cahoon, D. R., Guntenspergen, G. R., & Phelps, J. (2013). A global standard for monitoring coastal wetland vulnerability to accelerated sea-level rise. *Nature Climate Change*, *3*(5), 458–465. https://doi.org/10.1038/nclimate1756

Wellner, R., Beaubouef, R., Van Wagoner, J., Roberts, H., & Sun, T. (2005). Jet-plume depositional bodies—The primary building blocks of Wax Lake Delta. *Gulf Coast Association of Geological Societies Transactions*, *55*, 867–909.

Wolstencroft, M., Shen, Z., Törnqvist, T. E., Milne, G. A., & Kulp, M. (2014). Understanding subsidence in the Mississippi Delta region due to sediment, ice, and ocean loading: Insights from geophysical modeling. *Journal of Geophysical Research: Solid Earth*, *119*(4), 3838–3856. https://doi.org/10.1002/2013jb010928

Wright, L. D. (1977). Sediment transport and deposition at river mouths: A synthesis. *Geological Society of America Bulletin*, *88*, 857–868. https://doi.org/10.1130/0016-7606(1977)88<857:stadar>2.0.co;2

Yu, S.-Y., Törnqvist, T. E., & Hu, P. (2012). Quantifying Holocene lithospheric subsidence rates underneath the Mississippi Delta. *Earth and Planetary Science Letters*, *331*, 21–30. https://doi.org/10.1016/j.epsl.2012.02.021

Zoccarato, C., Minderhoud, P. S., & Teatini, P. (2018). The role of sedimentation and natural compaction in a prograding delta: Insights from the mega Mekong delta, Vietnam. *Scientific Reports*, *8*(1), 1–12. https://doi.org/10.1038/s41598-018-29734-7